ELSEVIER

Journal of Magnetism and Magnetic Materials 184 (1998) 145–154

Journal of magnetism and magnetic materials

Quantum effects in giant magnetoresistance due to interfaces in magnetic sandwiches

A. Vedyayev[a,*], M. Chshiev[a], B. Dieny[b]

[a] *Department of Physics, Moscow Lomonosov University, Moscow, 119899, Russian Federation*

[b] *CEA/Grenoble, Departement de Recherche Fondamentale sur la Matière Condensée, SP2M/NM, 38054, Grenoble, France*

Received 8 October 1997

Abstract

An analytical quantum-statistical theory of giant magnetoresistance (GMR) in magnetic sandwiches for current in-plane geometry (CIP) is developed taking into account quantization of electron motion perpendicular to plane direction and spin-dependent reflection and scattering of conduction electrons at interfaces. We adopted free electron model described by four parameters: mean free paths in the bulk and scattering amplitudes (coherent potentials) at interfaces for spin-up and spin-down electrons. The conductivities and GMR were calculated using Kubo formalism and Green functions technique in mixed real-space-mometum representation. Well-defined oscillations of CIP GMR with respect to thicknesses of the various layers due to the electron reflection on spin-dependent potential barriers at interfaces are predicted. The relative role of spin-dependent bulk and interfacial scattering and the influence of potential barriers at the interfaces on CIP GMR are investigated. © 1998 Elsevier Science B.V. All rights reserved.

PACS: 75.50.C; 72.15.C; 75.50.R

Keywords: Magnetic multilayers; Giant magnetoresistance

1. Introduction

The discovery of giant magnetoresistance (GMR) in Fe/Cr multilayers [1,2] and observation of this effect in many structures (multilayers or sandwiches F/P/F, where F and P indicate ferromagnetic layer and non-magnetic spacer, respectively) [3] triggered a large number of studies on GMR. It is widely agreed that the underlying mechanism of GMR is a coherent interplay of spin-dependent scattering of conduction electrons occurring at interfaces or in the bulk of the successive magnetic layers and electron reflection from spin-dependent potential barriers between layers. In earlier papers [4,5] it was considered that

* Corresponding auhor. Fax: + 7 095 932 8820; e-mail: vedy@vedy.phys.msu.su.

PII S0304-8853(97)01085-8

spin-dependent potential barriers are due to the exchange splitting of the electron bands in the bulk of the magnetic layers and no attention was paid to the reflection of electrons from narrow spin-dependent potential barriers existing only within the interface. In this paper we present a quantum-statistical theory of GMR for current in-plane (CIP) geometry. We consider a sandwich structure consisting of two ferromagnetic films separated by a metallic paramagnetic spacer with interfaces on the inner boundaries and infinite potential barriers on the outer boundaries. The interfaces are characterized by complex coherent potentials. Their real parts are responsible for the reflection of electrons from the interface whereas their imaginary parts describe the scattering of electrons on the interfaces. For calculation of the conductivity of the system, we used Kubo formalism and Green's functions method. For the adopted model we found the exact solution of the Dyson equation for the Green's function. Therefore, we took into account all effects due to the interference of electron waves reflected from the outer and inner (interface) boundaries.

2. Model

We consider the case of a sandwich (F_1 a/P b/F_2 c) consisting of two ferromagnetic layers F_1 and F_2 separated by a non-magnetic spacer P (a, b, c indicate the thicknesses of the respective layers). Within each layer, the electrons are described as a free electron gas subjected to scattering potentials located both in the bulk of the ferromagnetic layers and at the inner interfaces. No spin-flip scattering is taken into account. The electric current flows in the plane of the sample and the electron motion is constrained by infinite potential walls at the outer boundaries of the sandwich. The Kubo formula for CIP two-point conductivity $\sigma(z, z')$ may be written as follows [6]

$$\sigma(z, z') = \frac{e^2\hbar}{\pi N a_0^4} \sum_{\kappa,\mu} v_\kappa^2 G_\kappa^\mu G^{*\mu}_\kappa, \tag{1}$$

where $G_\kappa^\mu \equiv G_\kappa^\mu(z, z')$ and $G^{*\mu}_\kappa \equiv G^{*\mu}_\kappa(z, z')$ are retarded and advanced Green's functions of the electron system, μ indicates electron spin index $\uparrow(\downarrow)$, v_κ and κ the velocity operator and the electron's momentum in the XY-plane of the film, respectively, a_0 is the lattice constant, N the number of sites in the plane and z the direction perpendicular to the film's plane. Expression (1) is exact if one knows the exact Green's functions, but later we will use the expressions for the Green's functions averaged over the distribution of impurities in each XY monolayer. In this approach each individual layer (i) is characterized by its own coherent potential $\Sigma_i^{\uparrow(\downarrow)}$. For ferromagnetic layer Σ_i depends on the electron's spin $\uparrow(\downarrow)$. Further, we absorb spin index in the index i. The coherent potential is the solution of the equation [7]

$$x_i \frac{\varepsilon_i^{\mathrm{A}} - \Sigma_i}{1 - (\varepsilon_i^{\mathrm{A}} - \Sigma_i)(1/N)\sum_\kappa G_\kappa(z, z)} + (1 - x_i)\frac{\varepsilon_i^{\mathrm{B}} - \Sigma_i}{1 - (\varepsilon_i^{\mathrm{B}} - \Sigma_i)(1/N)\sum_\kappa G_\kappa(z, z)} = 0,$$

where we consider every layer i as an alloy $A_{x_i}B_{1-x_i}$ with random distribution of atoms type A(B) on the lattice sites. $\varepsilon_i^{\mathrm{A(B)}}$ are the on-site matrix elements of the potential of A(B) atoms, $(1/N)\sum_\kappa G_\kappa(z, z)$ is the diagonal on-site matrix element of the Green's function of the considered system. In the following, we consider only s-electrons with the same Fermi momentum. Consequently, for every layer, in the first approximation, we may take this latter matrix element as coinciding with its value in the corresponding bulk material. Moreover, we absorb the real part of the coherent potential into the value of the Fermi energy and take into account explicitely only its imaginary part $\mathrm{Im}\,\Sigma_i$, whose three values $\mathrm{Im}\,\Sigma^\uparrow \equiv \Sigma_1^b$, $\mathrm{Im}\,\Sigma^\downarrow \equiv \Sigma_3^b$ and $\mathrm{Im}\,\Sigma_p \equiv \Sigma_2^b$ are taken as the parameters of bulk scattering of spin $\uparrow(\downarrow)$ electrons in ferro- and paramagnetic layers ($\Sigma_p^\uparrow = \Sigma_p^\downarrow \equiv \Sigma_2^b$). Further, we introduce the spin-dependent coherent potentials $\mathrm{Re}\,\Sigma^\uparrow - \mathrm{i}\,\mathrm{Im}\,\Sigma^\uparrow \equiv \Sigma_1$ and $\mathrm{Re}\,\Sigma^\downarrow - \mathrm{i}\,\mathrm{Im}\,\Sigma^\downarrow \equiv \Sigma_2$ on the interfaces located at $z = a$ and $z = a + b$, where the real parts characterize the potential barriers at interfaces. As an example, for spin $\uparrow$ electrons and antiparallel orientation of

magnetizations in ferromagnetic layers, the Green's functions $G(z, z')$ (we omit spin index $\uparrow$) are the solutions of the equation

$$G(z, z') = G^0(z, z') + G^0(z, a)\Sigma_1 G(a, z') + G^0(z, a+b)\Sigma_2 G(a+b, z'), \tag{2}$$

where $G^0(z, z')$ is the solution of the equation

$$\left(\frac{\partial^2}{\partial z^2} - \kappa^2 + k_F^2 - 2\Sigma_i^b(z)\right) G^0(z, z') = \delta(z - z') \tag{3}$$

($\Sigma_i^b(z) = \Sigma_3^b$ for $0 < z < a$, $\Sigma_i^b(z) = \Sigma_2^b$ for $a < z < a+b$ and $\Sigma_i^b(z) = \Sigma_1^b$ for $a+b < z < a+b+c$) with boundary conditions $G^0(z'+\varepsilon, z') = G^0(z'-\varepsilon, z')$ and

$$\frac{\partial G^0(z'+\varepsilon, z')}{\partial z} - \frac{\partial G^0(z'-\varepsilon, z')}{\partial z} = a_0$$

when $\varepsilon = 0$. Also, $G^0(z, z') = 0$ at outer boundaries (for $z, z' = 0$ or $a+b+c$), $G^0(a+\varepsilon, z') = G^0(a-\varepsilon, z')$, $G^0(a+b+\varepsilon, z') = G^0(a+b-\varepsilon, z')$ and corresponding equalities for derivatives at inner boundaries. It is not worthwhile writing down here all solutions of Eq. (3). One can find them in Ref. [4]. As an example, in the region $0 < z, z' < a$ Green's function can be written as

$$G^0(z, z') = -\frac{1}{2\mathrm{i}k_0}\frac{1}{1 - \mathrm{e}^{2\mathrm{i}[k_3 a + k_2 b + k_1 c]}}\left[\mathrm{e}^{\mathrm{i}k_3(z+z')} + \mathrm{e}^{\mathrm{i}k_3(2a-z-z')}\mathrm{e}^{2\mathrm{i}(k_2 b + k_1 c)} - \mathrm{e}^{\mathrm{i}k_3|z-z'|}\right.$$
$$\left. - \mathrm{e}^{-\mathrm{i}k_3|z-z'|}\mathrm{e}^{2\mathrm{i}(k_3 a + k_2 b + k_1 c)}\right],$$

where $k_i = c_i + \mathrm{i}d_i = \sqrt{k_F^2 - \kappa^2 - 2\Sigma_i^b(z)} \equiv \sqrt{k_F^2 - \kappa^2 + \mathrm{i}2k_F/l_i(z)}$, l_i the elastic mean free path in the ith layer and $k_0 = \sqrt{k_F^2 - \kappa^2}$. It should be mentioned that we adopted $(2ma_0/\hbar^2) = 1$ and k_F as the Fermi momentum. The solution of Eq. (2) is

$$G(z, z') = G^0(z, z') + A_a G^0(z, a)G^0(a, z') + BG^0(z, a)G^0(a+b, z')$$
$$+ A_b G^0(z, a+b)G^0(a+b, z') + BG^0(z, a+b)G^0(a, z'), \tag{4}$$

where

$$A_a = \frac{\Sigma_1(1 - G^0(a+b, a+b)\Sigma_2)}{(1 - G^0(a, a)\Sigma_1)(1 - G^0(a+b, a+b)\Sigma_2) - G^0(a+b, a)\Sigma_1\Sigma_2 G^0(a, a+b)},$$

$$B = \frac{\Sigma_1 G^0(a, a+b)\Sigma_2}{(1 - G^0(a, a)\Sigma_1)(1 - G^0(a+b, a+b)\Sigma_2) - G^0(a+b, a)\Sigma_1\Sigma_2 G^0(a, a+b)}, \tag{5}$$

$$A_b = \frac{\Sigma_2(1 - G^0(a, a)\Sigma_1)}{(1 - G^0(a, a)\Sigma_1)(1 - G^0(a+b, a+b)\Sigma_2) - G^0(a+b, a)\Sigma_1\Sigma_2 G^0(a, a+b)}.$$

To proceed further we have to insert expressions (4) and (5) into (1) and calculate the two-point conductivity $\sigma(z, z')$ for spin-up and spin-down electrons for both parallel and antiparallel alignment of the magnetizations in the ferromagnetic layers. The current density at point z is given by

$$j(z) = \int \sigma(z, z')E(z')\,\mathrm{d}z', \tag{6}$$

where $E(z')$ is the electrical field at point z' assumed to lie along the x-axis. In the CIP geometry, the measured conductivity is given by

$$\sigma = \frac{1}{D}\int_0^D \int_0^D \mathrm{d}z\, \mathrm{d}z' \sigma(z, z'), \tag{7}$$

where $D = a + b + c$ is the total thickness of the sample. The final expression of this conductivity has been calculated analytically; its expression is given in the appendix. The expression of the magnetoresistance is obtained from the calculation of the conductivity in both parallel and antiparallel configurations of the magnetizations in successive ferromagnetic layers. In the next section, we use this analytical expression to investigate the relative role of spin-dependent scattering at interfaces and in the bulk of the ferromagnetic layers and the influence of potential barriers at interfaces on the GMR amplitude.

3. Results and discussion

3.1. Oscillations of GMR with thicknesses of the layers

As it follows from the expressions given in the appendix, the conductivity and GMR of multilayers oscillate as the thicknesses of the layers are varied. These oscillations due to the quantization of the z-component of the conduction electrons' momentum are caused by electron reflection on interfacial spin-dependent potential barriers. In Fig. 1, we plotted GMR effect for sandwich F 5 Å/P b/F 5 Å versus thickness of spacer b (b is varying from 3 to 20 Å) for different values of scattering parameters at the interfaces. The parameter $\lambda_s^{\downarrow(\uparrow)} = k_F a_0/\Sigma_{1(2)}$ indicates mean free path due to the scattering of spin down (up) electrons on an interface. The upper curve (curve 1) corresponds to the case where interfaces are absent. These weak observed oscillations are due to only the reflection of conduction electrons on outer boundaries [4,5]. In the cases of curves 2 and 4, respectively, weak and large spin-dependent potential steps are introduced at the interfaces between the magnetic and non-magnetic materials. These steps induce partial reflections of the electrons on

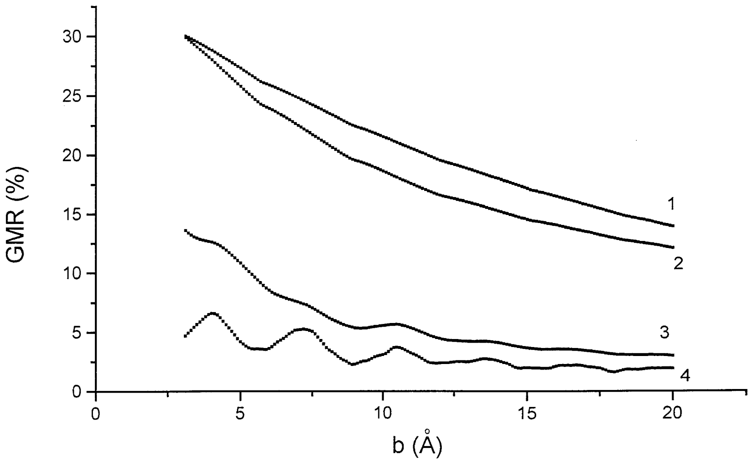

Fig. 1. CIP GMR of sandwich F 5 Å/P b Å/F 5 Å versus thickness b of paramagnetic spacer. The parameters are: $l_1/l_3 = 120$ Å/24 Å; $l_2 = 250$ Å; $k_F = 1$ Å^{-1}; $a_0 = 3$ Å; Re $\Sigma^\uparrow = 0$, Re $\Sigma^\downarrow = 0$, $\lambda_s^\uparrow = \lambda_s^\downarrow = \infty$ – curve 1; Re $\Sigma^\uparrow = 0.01$, Re $\Sigma^\downarrow = 0.1$, $\lambda_s^\uparrow = \lambda_s^\downarrow = \infty$ – curve 2; Re $\Sigma^\uparrow = 0.1$, Re $\Sigma^\downarrow = 1$, $\lambda_s^\uparrow = 200$, $\lambda_s^\downarrow = 10$ – curve 3; Re $\Sigma^\uparrow = 0.1$, Re $\Sigma^\downarrow = 1$, $\lambda_s^\uparrow = \lambda_s^\downarrow = \infty$ – curve 4.

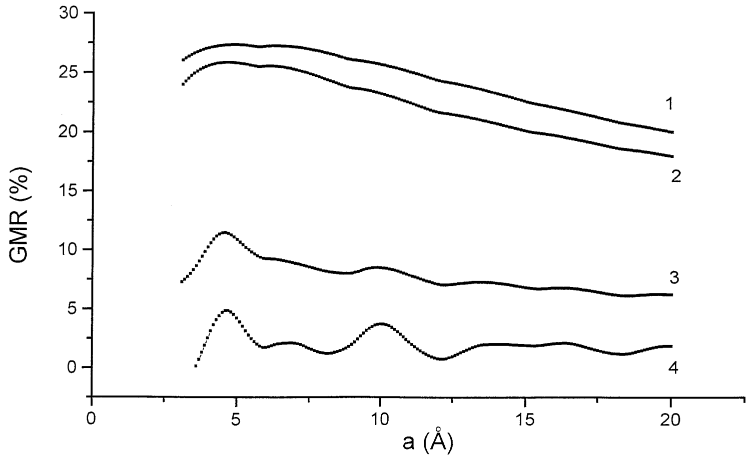

Fig. 2. CIP GMR of sandwich F a Å/P 5 Å/F 5 Å versus thickness a of ferromagnetic layer. The parameters are: $l_1/l_3 = 120$ Å/24 Å; $l_2 = 250$ Å; $k_F = 1$ Å^{-1}; $a_0 = 3$ Å; Re $\Sigma^\uparrow = 0$, Re $\Sigma^\downarrow = 0$, $\lambda_s^\uparrow = \lambda_s^\downarrow = \infty$ – curve 1; Re $\Sigma^\uparrow = 0.01$, Re $\Sigma^\downarrow = 0.1$, $\lambda_s^\uparrow = \lambda_s^\downarrow = \infty$ – curve 2; Re $\Sigma^\uparrow = 0.1$, Re $\Sigma^\downarrow = 1$, $\lambda_s^\uparrow = 200$, $\lambda_s^\downarrow = 10$ – curve 3; Re $\Sigma^\uparrow = 0.1$, Re $\Sigma^\downarrow = 1$, $\lambda_s^\uparrow = \lambda_s^\downarrow = \infty$ – curve 4.

inner interfaces, leading to more pronounced GMR oscillations with period π/k_F. However, the GMR amplitude tends to decrease as the height of the interfacial potential step increases. This is a general feature when the spin-dependent scattering in the bulk of the magnetic layers is large as in the present case. This decrease results from partial reflection of electrons on interfacial potential barriers resulting in weaker influence of the relative orientation of the magnetizations in the two ferromagnetic layers on the conductivity. Furthermore, curve 3 shows that including spin-dependent scattering at interfaces with scattering asymmetry $(\lambda_s^\uparrow - \lambda_s^\downarrow)/\lambda_s^\downarrow$ of the same sign than the bulk scattering asymmetry $(l_1 - l_3)/l_3$ leads to an increase in GMR amplitude with simultaneous decrease in the amplitude of oscillations. In the present case, the interfacial spin-dependent scattering reinforces the overall scattering contrast between the two species of electrons. This is not always the case. If the scattering asymmetry is opposite to the bulk one or if the electrons which have a long mean free path in the bulk of the ferromagnetic layers are strongly scattered at the interface (for instance, $\lambda_s^\uparrow = 20$ Å, $\lambda_s^\downarrow = 4$ Å), then the overall scattering contrast decreases, leading to a lower GMR amplitude than without interfacial scattering. Similar effects are observed in Fig. 2, where we plotted the dependence of GMR effect on the thickness of the ferromagnetic layer a for the same parameters as in Fig. 1. However, in this case, the presence of spin-dependent potential barriers at the interfaces leads to oscillations of a more complicated type, resulting from the mixing of two different periods, π/k_F and $2\pi/k_F$. These two periods originate from the interference of reflected electron waves, respectively, after having traversed one or two ferromagnetic layers. Here we have to mention that the dependence of conductivity on the thickness may be approximated by the single damping wave only in the case of homogeneous thin films. In the case under consideration this oscillatory behaviour has a more complicated form due to interference of electron waves reflected from all (outer and inner) boundaries.

3.2. *The relative importance of interfacial and bulk scattering*

In this section we consider the problem of relative importance of spin-dependent scattering occurring in the bulk and at the interfaces. To clarify this problem, we examine the GMR behaviour when scattering amplitude at the interfaces is changing. In Figs. 3–6 one can see the dependences of GMR versus $\lambda_s^\downarrow$ for fixed ratio $p_b = l_1/l_3$ and several values of $p_s = \lambda_s^\uparrow/\lambda_s^\downarrow$. Let us consider these dependences in detail.

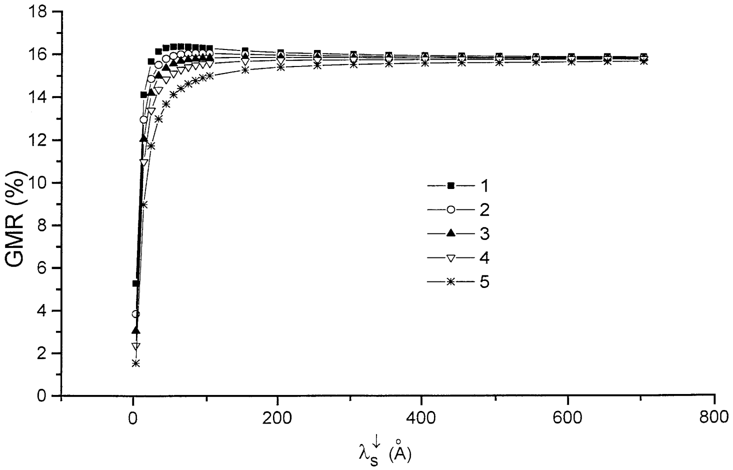

Fig. 3. CIP GMR of sandwich F 20 Å/P 10 Å/F 20 Å versus min mean free path $\lambda_s^{\downarrow}$ at interfaces ($\lambda_s^{\downarrow}$ varying from 3 upto 753 Å). The parameters are: $l_1/l_3 = 120$ Å/24 Å; $l_2 = 250$ Å; $k_F = 1$ Å^{-1}; $a_0 = 3$ Å; $\lambda_s^{\uparrow}/\lambda_s^{\downarrow} = 20$ – curve 1; $\lambda_s^{\uparrow}/\lambda_s^{\downarrow} = 10$ – curve 2; $\lambda_s^{\uparrow}/\lambda_s^{\downarrow} = 7$ – curve 3; $\lambda_s^{\uparrow}/\lambda_s^{\downarrow} = 5$ – curve 4; $\lambda_s^{\uparrow}/\lambda_s^{\downarrow} = 3$ – curve 5.

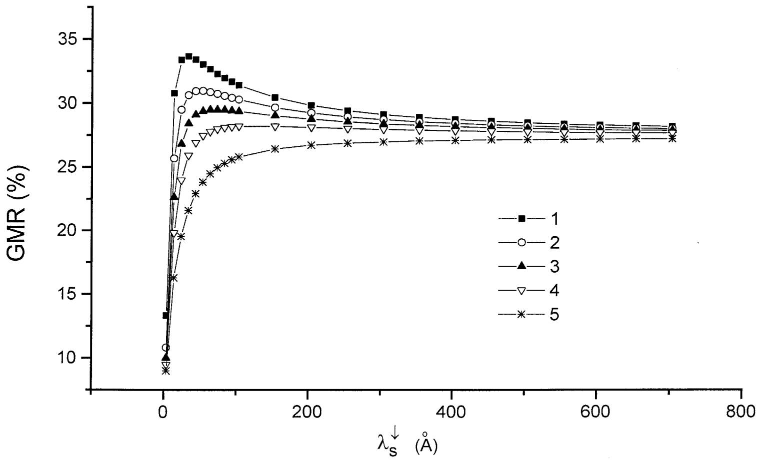

Fig. 4. CIP GMR of sandwich F 5 Å/P 5 Å/F 5 Å versus min mean free path $\lambda_s^{\downarrow}$ at interfaces ($\lambda_s^{\downarrow}$ varying from 3 upto 753 Å). The parameters are: $l_1/l_3 = 120$ Å/24 Å; $l_2 = 250$ Å; $k_F = 1$ Å^{-1}; $a_0 = 3$ Å; $\lambda_s^{\uparrow}/\lambda_s^{\downarrow} = 20$ – curve 1; $\lambda_s^{\uparrow}/\lambda_s^{\downarrow} = 10$ – curve 2; $\lambda_s^{\uparrow}/\lambda_s^{\downarrow} = 7$ – curve 3; $\lambda_s^{\uparrow}/\lambda_s^{\downarrow} = 5$ – curve 4; $\lambda_s^{\uparrow}/\lambda_s^{\downarrow} = 3$ – curve 5.

Fig. 3 corresponds to the case of a sandwich of the composition F 20 Å/P 10 Å/F 20 Å. The thickness of the ferromagnetic layer is here comparable to the shortest of the two mean free paths associated with spin-up and spin-down electrons (in the present case, this shortest mean free path is $\lambda_b^{\downarrow} = l_3$). As $\lambda_s^{\downarrow}$ decreases from infinity down to a few nanometers (which means that the interfacial scattering rate increases), the GMR amplitude almost does not vary. Since the thickness of the ferromagnetic layer is comparable or larger than $\lambda_b^{\downarrow}$, even without interfacial scattering, the spin-down electrons are scattered in the ferromagnetic layers whereas the spin-up electrons are not. The bulk spin-dependent scattering already ensures a great overall scattering contrast between the two species of electrons, thus leading to a large GMR amplitude. As the

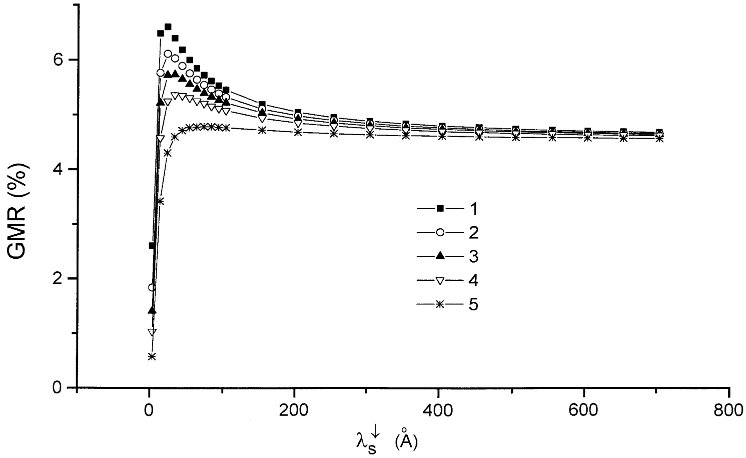

Fig. 5. CIP GMR of sandwich F 20 Å/P 10 Å/F 20 Å versus min mean free path $\lambda_s^{\downarrow}$ at interfaces ($\lambda_s^{\downarrow}$ varying from 3 upto 753 Å). The parameters are: $l_1/l_3 = 97$ Å/47 Å; $l_2 = 250$ Å; $k_F = 1$ Å^{-1}; $a_0 = 3$ Å; $\lambda_s^{\uparrow}/\lambda_s^{\downarrow} = 20$ – curve 1; $\lambda_s^{\uparrow}/\lambda_s^{\downarrow} = 10$ – curve 2; $\lambda_s^{\uparrow}/\lambda_s^{\downarrow} = 7$ – curve 3; $\lambda_s^{\uparrow}/\lambda_s^{\downarrow} = 5$ – curve 4; $\lambda_s^{\uparrow}/\lambda_s^{\downarrow} = 3$ – curve 5.

interfacial spin-dependent scattering increases, this additional scattering of spin-down electrons does not increase the GMR significantly because these electrons were already scattered in the bulk of the layers. However, if the interfacial scattering rate keeps on increasing ($\lambda_s^{\downarrow} \to 0$), the GMR drops significantly for $\lambda_s^{\uparrow} < \lambda_b^{\uparrow}$, i.e. for $\lambda_s^{\downarrow} < \lambda_b^{\uparrow}/p_s$ because the spin-up electrons which were not initially scattered in the ferromagnetic layers are now scattered at the F/P interfaces. This scattering of the spin-up electrons reduces the overall scattering contrast between the two species of electrons.

The situation is somewhat different in Fig. 4 which corresponds to thinner layers: F 5 Å/P 5 Å/F 5 Å. In this case, the ferromagnetic layers are thinner than $\lambda_b^{\downarrow}$, so that in the absence of interfacial scattering, the spin-down electrons are relatively weakly scattered in the ferromagnetic layers. If a strongly spin-dependent interfacial scattering is then introduced (curve 1 of Fig. 4), as $\lambda_s^{\downarrow}$ decreases from infinity, the first effect is to reinforce the scattering of the spin-down electrons, thus enhancing the overall scattering contrast and therefore the GMR. This is true to a certain value corresponding to $\lambda_s^{\uparrow} < \lambda_b^{\uparrow}$ below which the spin-up electrons become also strongly scattered, thus reducing the scattering contrast. On the contrary, if the interfacial scattering is weakly spin-dependent (curve 5 of Fig. 4), the increase in the scattering of spin-down electrons occurs approximately at the same rate as the increase in the scattering of spin-up electrons. There is therefore no gain in overall scattering contrast and therefore the GMR monotonically decreases as $\lambda_s^{\downarrow}$ decreases.

Figs. 5 and 6 show the same comparison for two different sets of thicknesses in the case of a weaker spin-dependent scattering in the bulk of the ferromagnetic layers ($\lambda_b^{\uparrow}/\lambda_b^{\downarrow} = 97$ Å/47 Å instead of 120 Å /24 Å in Figs. 3 and 4). In Fig. 5 and especially in Fig. 6, the spin-down electrons are weakly scattered in the bulk of the ferromagnetic layers. The additional interfacial scattering of these electrons then leads to a significant increase in the overall scattering contrast between the two species of electrons and therefore to a large enhancement in the GMR amplitude.

In conclusion, the interfacial spin-dependent scattering gives a significant contribution to the GMR when the scattering contrast in the bulk of the ferromagnetic layers is low either because the spin-scattering asymmetry $\lambda_b^{\uparrow}/\lambda_b^{\downarrow}$ is close to unity or because the ferromagnetic layers are much thinner than the shortest of the two mean free paths $\lambda_b^{\uparrow}$ or $\lambda_b^{\downarrow}$. Recently, Zhang and Levy [8] have shown that the spin dependence of scattering from correlated pairs at interfaces is enhanced compared to scattering in the bulk. At the same time

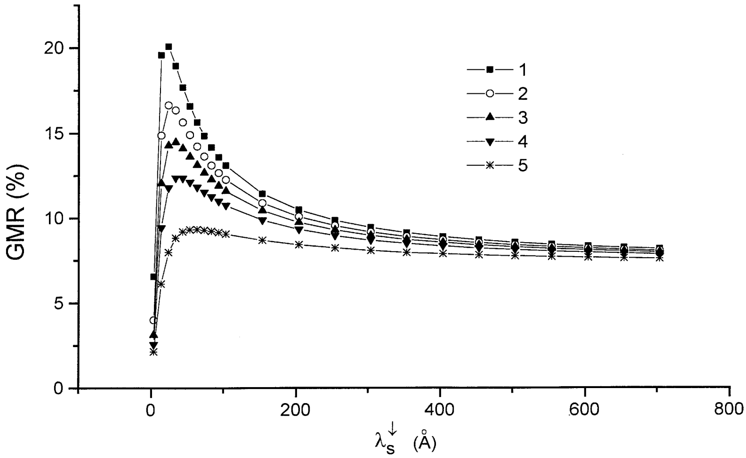

Fig. 6. CIP GMR of sandwich F 5 Å/P 5 Å/F 5 Å versus min mean free path $\lambda_s^{\downarrow}$ at interfaces ($\lambda_s^{\downarrow}$ varying from 3 upto 753 Å). The parameters are: $l_1/l_3 = 97$ Å /47 Å; $l_2 = 250$ Å; $k_F = 1$ Å^{-1}; $a_0 = 3$ Å; $\lambda_s^{\uparrow}/\lambda_s^{\downarrow} = 20$ – curve 1; $\lambda_s^{\uparrow}/\lambda_s^{\downarrow} = 10$ – curve 2; $\lambda_s^{\uparrow}/\lambda_s^{\downarrow} = 7$ – curve 3; $\lambda_s^{\uparrow}/\lambda_s^{\downarrow} = 5$ – curve 4; $\lambda_s^{\uparrow}/\lambda_s^{\downarrow} = 3$ – curve 5.

it follows from the above discussion that the scattering at interfaces gives essential contribution to GMR compared to one in the bulk only if the spin-dependent ratio at interfaces p_s is much larger than p_b. This situation corresponds to the correlation between the ratios of the spin-dependent scattering in the bulk and at interface obtained by Zhang and Levy (see Ref. [8] and Fig. 2 therein).

Lastly, we will try to explain the existence of a maximum in dependences of GMR on $\lambda_s^{\downarrow}$ discussed above (Figs. 3–6) from another point of view. In our previous work [9] we have shown that the coherent potential $\Sigma_{1(2)}$ of an isolated interface is renormalized to $\Sigma_{1(2)}^{\rm eff} = \Sigma_{1(2)}/(1 + \Sigma_{1(2)}/k_F)$. This renormalization has a clean physical interpretation: electron scattering on interface influences the total CIP conductivity and the contribution of the interface scattering to resistivity reaches the maximum for perfectly 'diffuse' scattering. In this regime an electron forgets its momentum history after scattering on the length $\sim k_F^{-1}$, and this length cannot be shorter for any value of the initial scattering potential $\Sigma_{1(2)}$. The ratio of renormalized interfacial coherent potentials for up- and down-spin electrons tends to unity with increasing of interfacial scattering. So the behaviour of GMR can be explained as follows: for large λ_s, $p_s^{\rm eff} = (\lambda_s^{\uparrow}(1 + a_0/\lambda_s^{\uparrow}))/(\lambda_s^{\downarrow}(1 + a_0/\lambda_s^{\downarrow})) \approx p_s > p_b$. So increasing the interfacial scattering gives additional contribution to total GMR, but for small λ_s, $p_s^{\rm eff}$ decreases and it may become smaller than p_b, therefore the additional interfacial scattering is less asymmetric in the direction of spin so that the GMR begins to decrease. In the case under consideration with two interfaces, this renormalization has a more complicated character due to mutual influence of interfaces scattering (see Eq. (4) and the appendix). Barnas and Bruynseraede [5] investigated the influence of interfacial scattering on CIP GMR and they obtained for $p_s > p_b$ a monotonic increase of GMR with the amplitude of interface roughness. But they consider the interfacial scattering only in Born approximation, so they missed the effect of renormalization discussed above.

Acknowledgements

This work was supported by the Russian fund for basic research (Grant N 96-02-19681a), INTAS (Grant N 93-0718) and NATO (Grant HTECH.LG 951527).

Appendix

In this appendix, an analytical expression for the conductivity of a sandwich (F a/P b/F c) with infinite potential walls on outer boundaries and with interfaces on inner boundaries is given. Using and transforming expressions (5) the following was obtained that

$$A_a = \frac{(1/k_0)\Sigma_1[\mathrm{den} - G^0(a+b, a+b)\Sigma_2]}{[\mathrm{den} - G^0(a,a)\Sigma_1][\mathrm{den} - G^0(a+b,a+b)\Sigma_2] - \Sigma_1\Sigma_2(G^0(a,a+b))^2},$$

$$B = \frac{(1/k_0)\Sigma_1\Sigma_2 G^0(a, a+b)}{[\mathrm{den} - G^0(a,a)\Sigma_1][\mathrm{den} - G^0(a+b,a+b)\Sigma_2] - \Sigma_1\Sigma_2(G^0(a,a+b))^2},$$

$$A_b = \frac{(1/k_0)\Sigma_2[\mathrm{den} - G^0(a,a)\Sigma_1]}{[\mathrm{den} - G^0(a,a)\Sigma_1][\mathrm{den} - G^0(a+b,a+b)\Sigma_2] - \Sigma_1\Sigma_2(G^0(a,a+b))^2},$$

where

$$\mathrm{den} = 1 - \mathrm{e}^{2\mathrm{i}k_3a}\mathrm{e}^{2\mathrm{i}k_2b}\mathrm{e}^{2\mathrm{i}k_1c},$$

$$G^0(a,a) = \frac{1}{2\mathrm{i}k_0}(1 - \mathrm{e}^{2\mathrm{i}k_2b}\mathrm{e}^{2\mathrm{i}k_1c})(1 - \mathrm{e}^{2\mathrm{i}k_3a}),$$

$$G^0(a,a+b) = \frac{1}{2\mathrm{i}k_0}\mathrm{e}^{\mathrm{i}k_2b}(1 - \mathrm{e}^{2\mathrm{i}k_3a})(1 - \mathrm{e}^{2\mathrm{i}k_1c}),$$

$$G^0(a+b,a+b) = \frac{1}{2\mathrm{i}k_0}(1 - \mathrm{e}^{2\mathrm{i}k_3a}\mathrm{e}^{2\mathrm{i}k_2b})(1 - \mathrm{e}^{2\mathrm{i}k_1c}).$$

Further, we introduce next terms

$$U_{aa} = \mathrm{i}[A_a(1 - \mathrm{e}^{2\mathrm{i}k_2b}\mathrm{e}^{2\mathrm{i}k_1c})^2 + 2B\mathrm{e}^{\mathrm{i}k_2b}(1 - \mathrm{e}^{2\mathrm{i}k_2b}\mathrm{e}^{2\mathrm{i}k_1c})(1 - \mathrm{e}^{2\mathrm{i}k_1c}) + A_b\mathrm{e}^{2\mathrm{i}k_2b}(1 - \mathrm{e}^{2\mathrm{i}k_1c})^2],$$

$$U_{ab} = 1 - \mathrm{i}[A_a(1 - \mathrm{e}^{2\mathrm{i}k_2b}\mathrm{e}^{2\mathrm{i}k_1c})(1 - \mathrm{e}^{2\mathrm{i}k_3a}) + B\mathrm{e}^{\mathrm{i}k_2b}(1 - \mathrm{e}^{2\mathrm{i}k_3a})(1 - \mathrm{e}^{2\mathrm{i}k_1c})],$$

$$\tilde{U}_{ab} = \mathrm{i}[A_b\mathrm{e}^{\mathrm{i}k_2b}(1 - \mathrm{e}^{2\mathrm{i}k_1c})^2 + B(1 - \mathrm{e}^{2\mathrm{i}k_1c})(1 - \mathrm{e}^{2\mathrm{i}k_2b}\mathrm{e}^{2\mathrm{i}k_1c})],$$

$$U^1_{bb} = \mathrm{e}^{2\mathrm{i}k_3a} + \mathrm{i}[A_a(1 - \mathrm{e}^{2\mathrm{i}k_3a})^2 - 2B\mathrm{e}^{\mathrm{i}k_2b}\mathrm{e}^{2\mathrm{i}k_3a}(1 - \mathrm{e}^{2\mathrm{i}k_3a})(1 - \mathrm{e}^{2\mathrm{i}k_1c}) + A_b\mathrm{e}^{2\mathrm{i}k_2b}\mathrm{e}^{4\mathrm{i}k_3a}(1 - \mathrm{e}^{2\mathrm{i}k_1c})^2],$$

$$U^2_{bb} = \mathrm{e}^{2\mathrm{i}k_1c} + \mathrm{i}[A_b(1 - \mathrm{e}^{2\mathrm{i}k_1c})^2 - 2B\mathrm{e}^{\mathrm{i}k_2b}\mathrm{e}^{2\mathrm{i}k_1c}(1 - \mathrm{e}^{2\mathrm{i}k_3a})(1 - \mathrm{e}^{2\mathrm{i}k_1c}) + A_a\mathrm{e}^{2\mathrm{i}k_2b}\mathrm{e}^{4\mathrm{i}k_1c}(1 - \mathrm{e}^{2\mathrm{i}k_3a})^2],$$

$$U^3_{bb} = \mathrm{i}[A_a\mathrm{e}^{2\mathrm{i}k_2b}\mathrm{e}^{2\mathrm{i}k_1c}(1 - \mathrm{e}^{2\mathrm{i}k_3a})^2 - B\mathrm{e}^{\mathrm{i}k_2b}(1 - \mathrm{e}^{2\mathrm{i}k_3a})(1 - \mathrm{e}^{2\mathrm{i}k_1c})(1 + \mathrm{e}^{2\mathrm{i}k_3a}\mathrm{e}^{2\mathrm{i}k_2b}\mathrm{e}^{2\mathrm{i}k_1c})$$
$$+ A_b\mathrm{e}^{2\mathrm{i}k_2b}\mathrm{e}^{2\mathrm{i}k_3a}(1 - \mathrm{e}^{2\mathrm{i}k_1c})^2],$$

$$U_{bc} = 1 - \mathrm{i}[A_b(1 - \mathrm{e}^{2\mathrm{i}k_2b}\mathrm{e}^{2\mathrm{i}k_3a})(1 - \mathrm{e}^{2\mathrm{i}k_1c}) + B\mathrm{e}^{\mathrm{i}k_2b}(1 - \mathrm{e}^{2\mathrm{i}k_3a})(1 - \mathrm{e}^{2\mathrm{i}k_1c})],$$

$$\tilde{U}_{bc} = \mathrm{i}[A_a\mathrm{e}^{\mathrm{i}k_2b}(1 - \mathrm{e}^{2\mathrm{i}k_3a})^2 + B(1 - \mathrm{e}^{2\mathrm{i}k_3a})(1 - \mathrm{e}^{2\mathrm{i}k_3a}\mathrm{e}^{2\mathrm{i}k_2b})],$$

$$U_{cc} = \mathrm{i}[A_b(1 - \mathrm{e}^{2\mathrm{i}k_2b}\mathrm{e}^{2\mathrm{i}k_3a})^2 + 2B\mathrm{e}^{\mathrm{i}k_2b}(1 - \mathrm{e}^{2\mathrm{i}k_2b}\mathrm{e}^{2\mathrm{i}k_3a})(1 - \mathrm{e}^{2\mathrm{i}k_3a}) + A_a\mathrm{e}^{2\mathrm{i}k_2b}(1 - \mathrm{e}^{2\mathrm{i}k_3a})^2],$$

$$U_{ac} = 1 - \mathrm{i}[A_a(1 - \mathrm{e}^{2\mathrm{i}k_2b}\mathrm{e}^{2\mathrm{i}k_1c})(1 - \mathrm{e}^{2\mathrm{i}k_3a}) + B\mathrm{e}^{\mathrm{i}k_2b}(1 - \mathrm{e}^{2\mathrm{i}k_3a})(1 - \mathrm{e}^{2\mathrm{i}k_1c})$$
$$+ A_b(1 - \mathrm{e}^{2\mathrm{i}k_2b}\mathrm{e}^{2\mathrm{i}k_3a})(1 - \mathrm{e}^{2\mathrm{i}k_1c}) + B\mathrm{e}^{-\mathrm{i}k_2b}(1 - \mathrm{e}^{2\mathrm{i}k_2b}\mathrm{e}^{2\mathrm{i}k_3a})(1 - \mathrm{e}^{2\mathrm{i}k_2b}\mathrm{e}^{2\mathrm{i}k_1c})],$$

$$\mathrm{Term}_1 = 1 + U_{aa}\mathrm{e}^{2\mathrm{i}k_3a} + [U_{aa}\mathrm{e}^{2\mathrm{i}k_3a}]^* - \mathrm{e}^{-4d_3a}\mathrm{e}^{-4d_2b}\mathrm{e}^{-4d_1c} - U^*_{aa}\mathrm{e}^{-4d_3a}\mathrm{e}^{2\mathrm{i}k_2b}\mathrm{e}^{2\mathrm{i}k_1c}$$
$$- U_{aa}[\mathrm{e}^{-4d_3a}\mathrm{e}^{2\mathrm{i}k_2b}\mathrm{e}^{2\mathrm{i}k_1c}]^*,$$

$$\mathrm{Term}_2 = 1 + U_{bb}^3 + [U_{bb}^3]^* - \mathrm{e}^{-4d_3a}\mathrm{e}^{-4d_2b}\mathrm{e}^{-4d_1c} - [U_{bb}^3]^*\mathrm{e}^{2\mathrm{i}k_3a}\mathrm{e}^{2\mathrm{i}k_2b}\mathrm{e}^{2\mathrm{i}k_1c} - U_{bb}^3[\mathrm{e}^{2\mathrm{i}k_3a}\mathrm{e}^{2\mathrm{i}k_2b}\mathrm{e}^{2\mathrm{i}k_1c}]^*,$$

$$\mathrm{Term}_3 = 1 + U_{cc}\mathrm{e}^{2\mathrm{i}k_1c} + [U_{cc}\mathrm{e}^{2\mathrm{i}k_1c}]^* - \mathrm{e}^{-4d_3a}\mathrm{e}^{-4d_2b}\mathrm{e}^{-4d_1c} - U_{cc}^*\mathrm{e}^{-4d_1c}\mathrm{e}^{2\mathrm{i}k_2b}\mathrm{e}^{2\mathrm{i}k_3a} - U_{cc}[\mathrm{e}^{-4d_1c}\mathrm{e}^{2\mathrm{i}k_2b}\mathrm{e}^{2\mathrm{i}k_3a}]^*,$$

$$\mathrm{Term}_4 = (1-\mathrm{e}^{-2d_3a})\{|1+U_{aa}\mathrm{e}^{2\mathrm{i}k_3a}|^2(1-\mathrm{e}^{-2d_3a}) + |U_{aa}+\mathrm{e}^{2\mathrm{i}k_2b}\mathrm{e}^{2\mathrm{i}k_1c}|^2(1-\mathrm{e}^{-2d_3a}) - 2(1+U_{aa}\mathrm{e}^{2\mathrm{i}k_3a} + [U_{aa}\mathrm{e}^{2\mathrm{i}k_3a}]^*) - 2|U_{aa}|^2\mathrm{e}^{-4d_3a}(1-\mathrm{e}^{2d_3a})\} - 2(1-\mathrm{e}^{2d_3a})\{\mathrm{e}^{-4d_3a}\mathrm{e}^{-4d_2b}\mathrm{e}^{-4d_1c} + U_{aa}^*\mathrm{e}^{-4d_3a}\mathrm{e}^{2\mathrm{i}k_2b}\mathrm{e}^{2\mathrm{i}k_1c} + U_{aa}[\mathrm{e}^{-4d_3a}\mathrm{e}^{2\mathrm{i}k_2b}\mathrm{e}^{2\mathrm{i}k_1c}]^*\},$$

$$\mathrm{Term}_5 = (1-\mathrm{e}^{-2d_2b})\{(|U_{bb}^1|^2 + |U_{bb}^2|^2)(1-\mathrm{e}^{-2d_2b}) - 2(1+U_{bb}^3+[U_{bb}^3]^*) - 2|U_{bb}^3|^2(1-\mathrm{e}^{2d_2b})\} - 2(1-\mathrm{e}^{2d_2b})\{\mathrm{e}^{-4d_3a}\mathrm{e}^{-4d_2b}\mathrm{e}^{-4d_1c} + [U_{bb}^3]^*\mathrm{e}^{2\mathrm{i}k_3a}\mathrm{e}^{2\mathrm{i}k_2b}\mathrm{e}^{2\mathrm{i}k_1c} + U_{bb}^3[\mathrm{e}^{2\mathrm{i}k_3a}\mathrm{e}^{2\mathrm{i}k_2b}\mathrm{e}^{2\mathrm{i}k_1c}]^*\},$$

$$\mathrm{Term}_6 = (1-\mathrm{e}^{-2d_1c})\{|1+U_{cc}\mathrm{e}^{2\mathrm{i}k_1c}|^2(1-\mathrm{e}^{-2d_1c}) + |U_{cc}+\mathrm{e}^{2\mathrm{i}k_2b}\mathrm{e}^{2\mathrm{i}k_3a}|^2(1-\mathrm{e}^{-2d_1c}) - 2(1+U_{cc}\mathrm{e}^{2\mathrm{i}k_1c} + [U_{cc}\mathrm{e}^{2\mathrm{i}k_1c}]^*) - 2|U_{cc}|^2\mathrm{e}^{-4d_1c}(1-\mathrm{e}^{2d_1c})\} - 2(1-\mathrm{e}^{2d_1c})\{\mathrm{e}^{-4d_3a}\mathrm{e}^{-4d_2b}\mathrm{e}^{-4d_1c} + U_{cc}^*\mathrm{e}^{-4d_1c}\mathrm{e}^{2\mathrm{i}k_2b}\mathrm{e}^{2\mathrm{i}k_3a} + U_{cc}[\mathrm{e}^{-4d_1c}\mathrm{e}^{2\mathrm{i}k_2b}\mathrm{e}^{2\mathrm{i}k_3a}]^*\},$$

$$\mathrm{Term}_7 = (1-\mathrm{e}^{-2d_2b})(1-\mathrm{e}^{-4d_3a})\{|U_{ab}+\mathrm{e}^{2\mathrm{i}k_3a}\mathrm{e}^{\mathrm{i}k_2b}\tilde{U}_{ab}|^2 + |U_{ab}\mathrm{e}^{\mathrm{i}k_2b}\mathrm{e}^{2\mathrm{i}k_1c} + \tilde{U}_{ab}|^2\},$$

$$\mathrm{Term}_8 = (1-\mathrm{e}^{-2d_2b})(1-\mathrm{e}^{-4d_1c})\{|U_{bc}+\mathrm{e}^{2\mathrm{i}k_1c}\mathrm{e}^{\mathrm{i}k_2b}\tilde{U}_{bc}|^2 + |U_{bc}\mathrm{e}^{\mathrm{i}k_2b}\mathrm{e}^{2\mathrm{i}k_3a} + \tilde{U}_{bc}|^2\},$$

$$\mathrm{Term}_9 = (1-\mathrm{e}^{-4d_3a})(1-\mathrm{e}^{-4d_1c})|U_{ac}|^2\mathrm{e}^{-2d_2b}.$$

Finally, we obtained the expression for antiparallel conductivity for spin-up electrons

$$\sigma_{\mathrm{AP}}^{\uparrow} = \frac{3}{16}\frac{C}{D}\frac{1}{|\mathrm{den}|^2}\int_0^1 x\,\mathrm{d}x\left\{4k_{\mathrm{F}}a\frac{l_3}{c_3}\mathrm{Term}_1 + 4k_{\mathrm{F}}b\frac{l_2}{c_2}\mathrm{Term}_2 + 4k_{\mathrm{F}}c\frac{l_1}{c_1}\mathrm{Term}_3 + l_3^2\,\mathrm{Term}_4 + l_2^2\,\mathrm{Term}_5 + l_1^2\,\mathrm{Term}_6 + 2l_2l_3\,\mathrm{Term}_7 + 2l_1l_2\mathrm{Term}_8 + 2l_1l_3\,\mathrm{Term}_9\right\}.$$

References

[1] M.N. Baibich et al., Phys. Rev. Lett. 61 (1988) 2472.
[2] G. Binash et al., Phys. Rev. B 39 (1989) 4828.
[3] B. Dieny, J. Magn. Magn. Mater. 136 (1994) 335.
[4] A. Vedyayev, C. Cowache, N. Ryzhanova, B. Dieny, J. Phys.: Condens. Matter 5 (1993) 8289.
[5] J. Barnas, Y. Bruynseraede, Phys. Rev. B 53 (9) 1996.
[6] A. Vedyayev, B. Dieny, N. Ryzhanova, Europhys. Lett. 19 (1992) 329.
[7] H. Ehrenreich, L. Schwartz, The Electronic Structure of Alloys, Solid State Physics, vol. 31, Academic Press, New York, 1976.
[8] S. Zhang, P.M. Levy, Phys. Rev. Lett. 77 (1996) 916.
[9] A. Vedyayev, M. Chshiev, N. Ryzhanova, B. Dieny, C. Cowache, F. Brouers, J. Magn. Magn. Mater. 172 (1997) 53.